OptiGap: A Modular Optical Sensor System for Bend Localization

Paul Bupe, Jr.[1], C. K. Harnett[1]

***Abstract*— This paper presents the novel use of air gaps in flexible optical light pipes to create coded patterns for use in bend localization. The OptiGap sensor system allows for the creation of extrinsic intensity modulated bend sensors that function as flexible absolute linear encoders. Coded air gap patterns are identified by a Gaussian naive Bayes (GNB) classifier running on an STM32 microcontroller. The fitting of the classifier is aided by a custom software suite that simplifies data collection and processing from the sensor. The sensor model is analyzed and verified through simulation and experiments, highlighting key properties and parameters that aid in the design of OptiGap sensors using different light pipe materials and for various applications. The OptiGap system allows for real-time and accurate bend localization in many robotics and automation applications, in both wet and dry conditions.**

I. Introduction

Soft optical deformation sensors make a good partner with soft robotics because their mechanical properties match, their materials are compatible with rapid prototyping, and they are less susceptible than electronic sensors to electromagnetic noise and temperature drift. However, options for localizing the deformation are lacking. In a previous work [1] we discussed a new class of soft robots consisting of Soft, Curved, Reconfigurable, Anisotropic Mechanisms, or SCRAMs [2]–[5]. We introduced and demonstrated the Thermally-Activated SCRAM Limb (TASL), a SCRAM device that can create virtual joints along a continuum curved sheet made of denim and PET plastic by creating a surface weakness along the curve using SMA wire that is embroidered into the sheet [1]. One shortcoming of the TASL was the lack of a bending sensor to verify that a joint formed at the desired location. This specifically required a bend sensor that was soft, small, and flexible enough to embed into a surface. In this paper, we present the optical gap (OptiGap) bend localization sensor system, a novel soft optical sensor system that is low cost, flexible, simple to fabricate, and able to perform real-time bend localization on almost any modern microcontroller.

A. Fiber Optic Sensors

Fiber optic sensors (FOS) typically consist of three components: a light source, a fiber light pipe that carries light and can be modulated, and a photodetector. FOS can be classified as either intrinsic or extrinsic. Intrinsic sensors have the sensing components integrated into the fiber such that the light is always contained and modulated within the fiber while extrinsic sensors have external sensing components that modulate that light, with the fiber acting primarily as a light pipe [6], [7]. FOS can also be categorized by whether they modulate the wavelength, polarization, phase, intensity, or a combination of those. Phase and intensity modulation sensors are by far the most common [7].

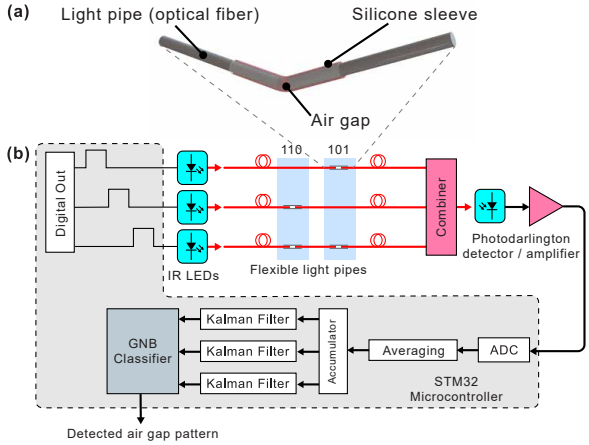

Fig. 1. **Overview of the OptiGap sensor system.** (a) Construction of the air gap used to create bend-sensitive areas in the light pipe. (b) Block diagram of the OptiGap system showing the optical emitters and detector, the fibers with bend-sensitive gaps, and the internal block diagram of the STM32 microcontroller that handles classification of the detected air gap patterns.

Using this taxonomy, OptiGap sensors can be considered extrinsic intensity modulated FOS. As shown in Fig. 1b the sensor system has three main components: IR LED emitters, flexible parallel light pipes, and a photodarlington detector. The light pipes all terminate into a single detector and the number of light pipes is variable, depending on the desired configuration of the sensor. Bend sensitivity is created at desired locations by cutting the light pipe and then re-attaching the pieces together using a sleeve to create a small air gap, shown in Fig. 1a. This is done on each of the multiple light pipes in order to create the air gap patterns (or codes) used for bend localization.

B. OptiGap Bend-Sensitive Air Gaps

OptiGap creates bend-sensitive air gaps along a piece of fiber by concentrating the mechanical deformation to a predetermined location. This is achieved by cutting the fiber perpendicular to the fiber axis and then re-attaching it together using soft silicone tubing while leaving a small air gap. The simulation and model in Fig. 2 shows the main working principle of the air gap: translation and/or rotation

This work is supported by the National Science Foundation [NSF Award #1935324]

[1] Department of Electrical and Computer Engineering, University of Louisville, Louisville, KY, 40292 USA

Corresponding author: C. K. Harnett (e-mail: c0harn01@louisville.edu)

of one fiber face relative to the other changes the fraction of light transmitted across the gap. The greater the bend angle the more light escapes across the gap. The resulting change in intensity of the optical signal is then correlated with known deformation for use as a sensor.

C. Existing Approaches

The concept of using a gap in fiber for intensity modulation can be found in literature. For a gap created by making a slice perpendicular to the fiber axis, a simple 2-dimensional model can be used where a circular fiber face is translated across another face and the overlap area gives the amount of transmission. This type of model is used in [8]–[10] and is used to describe bending [8], [9] and pressure [10] induced changes in optical intensity. The sensor in [8] uses one input fiber and two output fibers to measure bending in flexion and extension with an LED source at one end and a photodetector at the other end. Similarly, [9] uses one input fiber and three output fibers separated by a gap. This allows for measuring flexion, extension, and lateral planes. Both of these sensors have a single sensitive area and provide no information on bending location. Lin et al. [10] measure pressure by correlating the increase in optical intensity as the faces of two fibers align due to an external force.

Other similar non-gap approaches exist to measure bending and pressure [11], [12]. Zhao et el. create a curve sensor by bending a $1\,\mathrm{mm}$ acrylic fiber into a U-shape and roughening one side with a laser cutter in order to increase optical bending losses [11]. However, this sensor cannot provide information on bend location, motivating the same group to investigate wavelength-based encoding of the deformation site, leading to the SLIMS sensor [13]. The SLIMS sensor relies on color dyes in polyurethane elastomers and color sensors to detect bend locations, which makes the fabrication process complex, material selection limited, and imposes a centimeter-length limitation [13], unlike OptiGap. The pressure sensor in [12] consists of a pressure sensing sheet that is made of intersecting rows and columns of fiber encased in PDMS, each with an emitter and detector. A map of displacement and/or force over an area is generated by the intensity modulation caused by the bending of the fibers [12].

D. Primary Contributions

Our primary contributions in this paper are

1) A novel method of using an air gap with a sleeve, shown in Fig. 2, to produce coded bend-sensitive air gap patterns in optical light pipes through simple cutting without requiring sophisticated equipment.
2) An adaptation of the traditional robotics concept of linear encoders and Gray codes to a flexible soft optics sensor.
3) A low-cost and reconfigurable sensor system that is fast, can be made from various materials, and can be quickly customized for specific applications.

For the remainder of this paper, we first give an explanation of the operating principles of the OptiGap system in Section II-A, discuss the fabrication and signal processing steps in Sections II-B and II-C, and then delve into the use of a Gaussian naive Bayes (GNB) classifier in Section II-D. Finally, we cover the testing methodology, results, and discussion in Section III before concluding in Section IV.

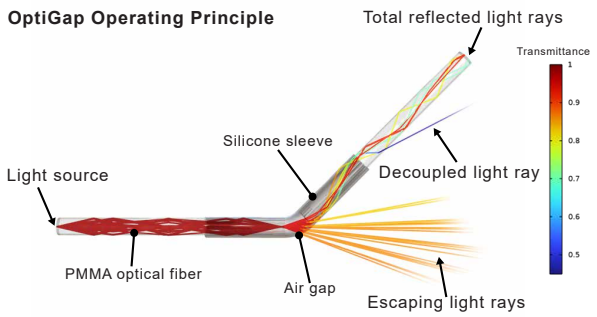

Fig. 2. A ray optics model and simulation of the bend-sensitive air gap used in OptiGap sensors. This model is bent at a $45°$ angle with a $15°$ cone angle light source and shows a significant amount of light escaping at the gap.

II. Methods

A. Operating Principles

The OptiGap sensor can best be thought of as a flexible absolute linear encoder. A linear encoder measures the linear displacement of an object and typically consists of a slider rail with a coded scale (much like a measuring ruler) and a sensing head that slides over that scale and reads the scale. The reading of the scale can be done by magnetic, optical, capacitive, resistive, ultrasonic, inductive, or mechanical means [14]. Absolute encoders output a unique pulse code at each step so the displacement relative to some scale is always known. More intuitively, an absolute encoder can be thought of as a ruler with the numbers and tick marks present while an incremental encoder is the same ruler with tick marks but no numbers. Similar to an absolute encoder, the OptiGap system can encode absolute positions using bend-sensitive air gap patterns along parallel light pipes as a FOS. The pattern of these bend-sensitive air gaps used to encode the bend location follows an n-bit binary sequence, where n is the number of parallel paths.

1) n-bit Inverse Gray Code: Gray code is a sequence of n-bit binary numbers where only a single bit is changed when transitioning from one number to the next, which can also be thought of as the Hamming distance between two adjacent numbers in the sequence is 1 [15]. As shown in the first column of Table I, this can be a form of built-in error detection since a change of more than one bit in the sequence has to be an error, which is why Gray code is often used as the coding for encoders as well as many communications applications.

Since the OptiGap system relies on a GNB classifier to identify the active air gap pattern we need to maximize the information gain from one pattern to the next, which is the opposite of what Gray code does. Inverse Gray code is where two adjacent n-bit numbers in the sequence differ by $n-1$

TABLE I

3-BIT GRAY CODE SEQUENCES

Number	Gray code	Inverse Gray code
0	000	000
1	001	110
2	011	011
3	010	101
4	110	010
5	111	100
6	101	001
7	100	111

bits, which is the maximum number of bits that can change in a binary sequence. A 3-bit example of this inverse Gray code is shown in the second column of Table I and was generated using the technique proposed in [16].

2) Sensor Array Gap Pattern: Each air gap pattern on an OptiGap sensor array can be thought of as an n-bit binary word in an inverse Gray code sequence. The inverse Gray code of number 1 in Table I corresponds with the first vertical pattern of air gaps in Fig. 3b. Similarly, number 7 in Table I corresponds with the last vertical pattern of air gaps. When a bend happens at an air gap pattern, the attenuation in optical intensity results in the bit pattern shown in Fig. 3c and is similar to the pulse pattern generated by an absolute encoder. Unlike an encoder, the real intensity signals, shown in Fig. 3d, are not consistent enough to directly convert to a binary signal, which is why the GNB classifier explained in Section II-D is used. Finally, each n-fiber sensor is limited to $2^n - 1$ sensitive patterns due to each pattern being equivalent to a binary word.

B. Fabrication

TABLE II

OPTIGAP CONFIGURATIONS TESTED

Length (m)	Material	Diameter (mm)	Air Gap Patterns
1.1 (Sensor A)	PMMA (fiber)	0.5	7
1.3 (Sensor B)	PMMA (fiber)	0.75	7
0.7 (Sensor C)	TPU (filament)	1.75	3

Because OptiGap is not a singular sensor but rather an adaptable *sensor system*, fabrication of any one sensor is entirely dependent on the application for that particular sensor. This is especially true of the placement of the bend-sensitive air gap patterns. While the system shown in Fig. 3 has evenly spaced air gap patterns for the sake of comparison with the illustrations, the air gap patterns can be placed anywhere along the length of the light pipes, much like the gratings in fiber Bragg grating (FBG) sensors.

Table II shows the system of Fig. 3 can be built from different diameter fibers and optical fiber materials. For PMMA fibers, the optical "combiner" in Fig. 3 consists of the three fibers in a silicone tube, connected to the optical detector. Since the TPU fibers are bigger, the combiner is a commercial 3:1 optical fiber combiner (Industrial Fiberoptics part 97638-001, Industrial Fiberoptics Inc). With that in

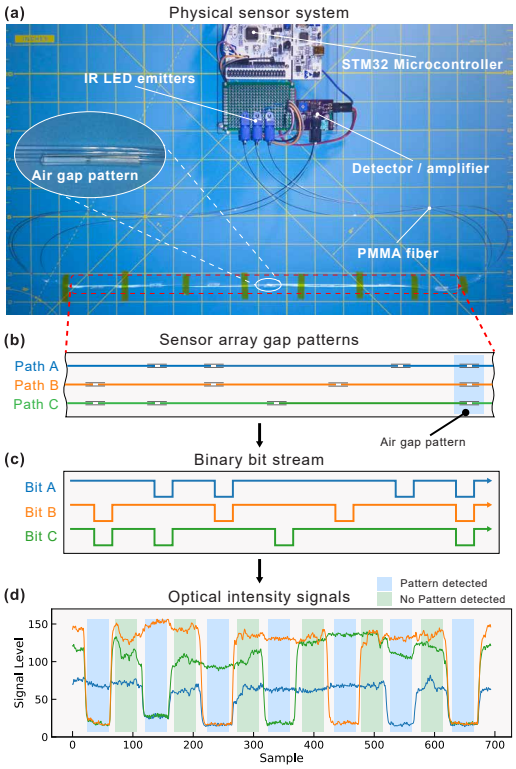

Fig. 3. **An OptiGap sensor with a visual explanation of the sensor operation.** (a) All the physical components of an OptiGap sensor including the emitters and detector, the microcontroller, and the fibers with the sensor array gap pattern. (b) The air gap pattern form bit patterns equivalent to an inverse Gray code binary word sequence that translates to (c) a corresponding bit stream pattern similar to an encoder pattern. (d) Since the real-world bit stream is not a consistent absolute signal, a GNB classifier is used to identify the active patterns.

mind, we highlight a number of key properties that affect the behavior and usability of an OptiGap sensor for different applications. These properties are also summarized in Table III.

1) Light Pipe Material: The light pipe material is the most important property because it greatly influences the total length of the sensor, the flexibility of the sensor, and the ability of the sensor to be embedded in various media. The chosen light pipe needs to have a very optically clear core with good flexibility. We have found PMMA fiber to be the most versatile light pipe due to its great optical properties, availability in various diameters, and general flexibility without breaking. Specifically, we used part numbers CK-20 and CK-30 from Industrial Fiber Optics with nominal diameters of $0.5\,\mathrm{mm}$ and $0.75\,\mathrm{mm}$, respectively. Both fibers have a fluorinated polymer cladding, a core refractive index of 1.49, and a numerical aperture of 0.5.

2) Air Gap Sleeve Material: The material covering the air gap needs to be soft enough to allow bending to occur at the gap but not too soft that it crumples easily. We found this ideal softness to equate to a Shore hardness of about 55A. The diameter of the sleeve material is not critical as long as it is smaller than the light pipe diameter so that it can firmly grip it. Our testing found that high-temperature silicone

tubing, such as McMaster-Carr part numbers 51845K66 and 51845K67, perfectly satisfies these requirements.

3) Optical Source, Detector, and Microcontroller: The choice of optical source and detector is not as critical as the previously mentioned design considerations, which is one of the strengths of this system. While any type of light source can be used in an OptiGap sensor, light in the IR spectrum is preferred for most sensor applications. Because of the gaps created in the light pipes, it is possible for ambient light to enter the system and raise the overall optical noise floor. Using a light source and detector in the IR spectrum provides much-needed immunity to ambient light, allowing the sensor to work in more conditions. The primary requirement for the microcontroller is for it to have an analog-to-digital converter (ADC) and as many digital outputs as optical paths in the sensor.

C. Signal Processing

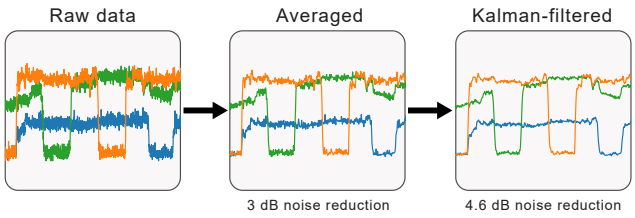

Fig. 4. The signal processing stages for noise reduction of the input signal. First, the signal is averaged, which produces a 3 dB noise reduction, and then it is Kalman-filtered for an additional 4.6 dB noise reduction.

Before being sent to the GNB classifier, the signals go through a two-stage noise reduction signal processing chain shown in Fig. 4. First, a simple averaging filter given by

$$\bar{A} = \frac{1}{n}\sum_{i=1}^{n} a_i$$

where n is the number of values to be averaged, is applied to the data. This filter serves both to smooth the raw data as well as stabilize the readings for the classifier by providing a slight delay. After the initial smoothing, a Kalman filter is used to further reduce the remaining signal noise without introducing any significant delay in the signal chain. A Kalman filter is an optimal and recursive algorithm that can estimate a target value using both a current measurement as well as the *a priori* knowledge about the system [17]. These filters are especially suitable for this application due to both being computationally efficient and simple enough to run on a microcontroller.

D. Classification

1) Naive Bayes Classifier: A GNB classifier is a supervised learning algorithm based on Bayes' theorem that determines how a measurement can be assigned to a particular class, C_i, assuming each class follows a Gaussian (normal) distribution with a certain probability $P(C_i)$. The *naive* part of the name assumes independent random variables. The operation of the GNB classifier hinges on two key questions: (1) How can a measurement, x, be assigned to class C_i for a given distribution? (2) What is the probability of error in that assignment?

The answer to the first question has an intuitive start: given any number of classes, a measurement should *most likely* belong to the class that has the highest probability of occurring. This means that, assuming the class follows a Gaussian distribution, a measurement x belongs to class $C_i, \in [1, M]$ when

$$max\Big\{ f_x(x|C_i)P(C_i) \quad \forall \quad i \in [1, M] \Big\}$$

with the Gaussian probability density function given by [18]

$$P(x|C_i) = \frac{1}{\sqrt{2\pi\sigma_{c_i}}} \exp\left(-\frac{(x-\mu_{c_i})}{2\sigma_{c_i}} \right)^2 \tag{1}$$

Addressing the second question, the probability of error is the probability of a measurement, x, from one class being misclassified as belonging to a different class. Given a two-class problem, the total probability of error is defined as

$$\begin{aligned} P_{err} = P(x|C_2)P(C_2)\ x \in C_1 \\ +P(x|C_1)P(C_1)\ x \in C_2 \end{aligned} \tag{2}$$

A GNB was used because it is more efficient than if-statements or lookup tables, can handle new or previously unseen data, and can be more accurate by taking into account the relationships between multiple input variables.

2) Fitting and Prediction: Fitting of the training data to a usable GNB classifier was performed using the GaussianNB module of the popular Scikit-learn Python library. In order to fit the model, data for each air gap pattern had to be captured from the sensor, labeled appropriately, then sent to the GaussianNB module. The output of the fitting process was a set of parameters representing the various Gaussian distributions and probabilities for each pattern as determined by the sensor data. The actual prediction was performed by a GNB classifier on the STM32 microcontroller, implemented using the Arm CMSIS-DSP C library which contains common signal processing functions. This allowed the microcontroller to perform real-time predictions while offloading the compute-intensive fitting process to a desktop computer.

III. Results and Discussion

Our testing methodology was to first validate our model and proposed air gap concept through simulation using COMSOL Multiphysics and then physically build, characterize, and test variations of the system. We utilized ray optics simulations instead of wave optics because the OptiGap system is designed to operate with multiple materials – the fiber is treated as a generic light pipe and is not material-dependent.

We simulated the bending of a piece of PMMA fiber with an air gap of $1\,\mathrm{mm}$ and of $2\,\mathrm{mm}$ then simulated the bending of a piece of fiber with no air gap, for reference. To account for different types of light source lenses, we also studied through simulation the effects of changing the cone angle of

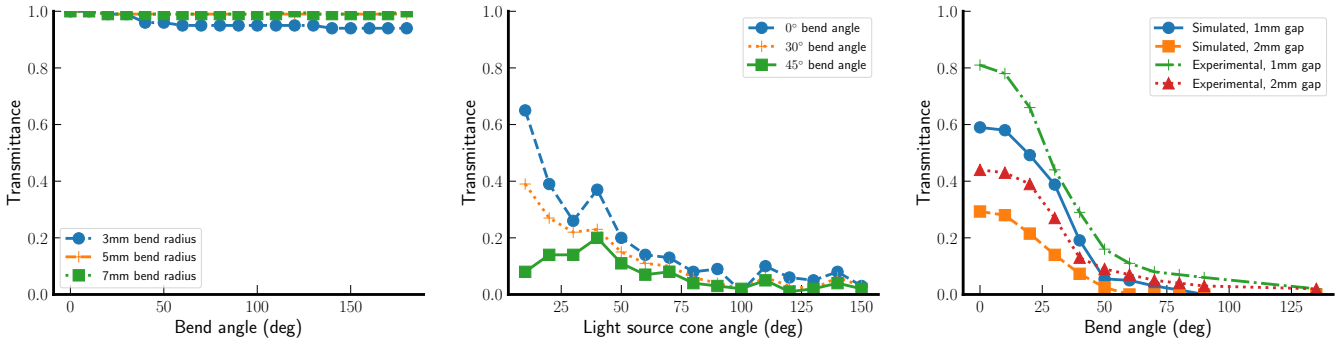

(a) Bend angle vs transmittance (b) Source cone angle vs transmittance (c) Gap bend angle vs transmittance

Fig. 5. **Simulation and experimental results.** (a) The effects of bending a 1 mm piece of PMMA fiber on transmittance. A minimal drop-off starts at around 40°. (b) The cone angle of the light source has a noticeable impact on transmittance. The smaller the cone angle the higher the transmittance. There is extra sensitivity at 40° during the downward trend. (c) A comparison of simulated and experimental data of the bend angle and transmittance. The simulation and experimental data follow the same curves even though the experimental data has a higher offset.

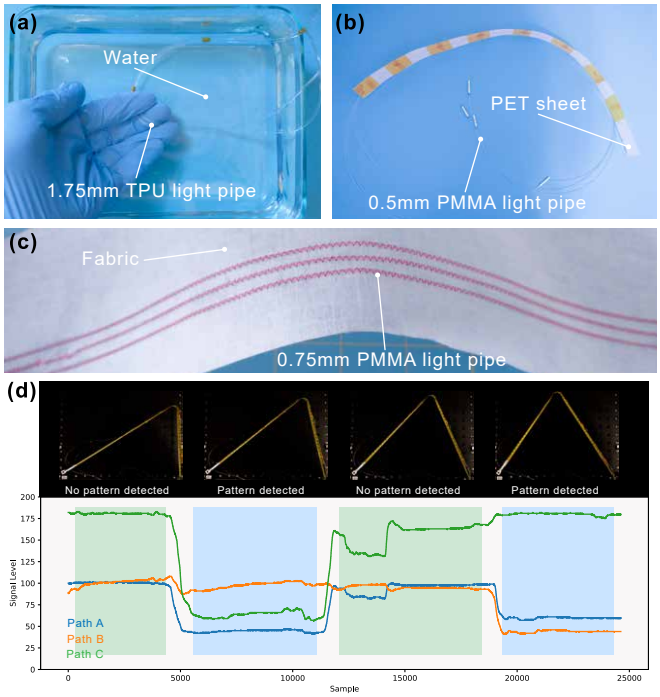

Fig. 6. **Experimental setup and results.** (a) OptiGap sensor working underwater. (b) The sensor attached to PET. (c) OptiGap light pipes embroidered into fabric. (d) 0.5 mm PMMA sensor attached to a tape spring testing rig showing how the bend location corresponds to the air gap pattern.

the light source. To experimentally test the bending of the fiber, we drew and printed a CAD pattern that contained outlines of all the test bend angles. We then aligned the fiber on top of the paper for each bend angle, allowing for consistent and repeatable testing. For all these tests we used transmittance as the primary metric, which is given by

$$T = \frac{I}{I_0} \tag{3}$$

and is the ratio of transmitted light to incident light.

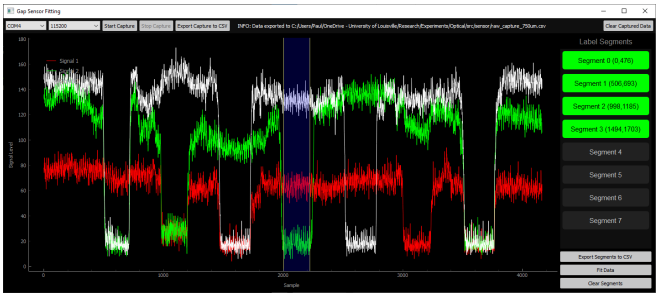

Fig. 7. The initial version GUI created to facilitate fast testing, labeling, and fitting of data for the OptiGap system.

A. *Bend Angle*

The air gap significantly reduces transmittance as the bend angle increases. Bending a fiber with no air gap results in minimal loss of light as the simulation in Fig. 5a shows. For the smallest 3 mm bend angle, a 180° bend resulted in only a 6% drop in transmittance. Conversely, adding an air gap results in a 75% drop by 50° and effectively a total loss in transmittance by 125°, which is shown in Fig. 5c. The experimental results in the same figure match the simulation in terms of percentage drop. For both experimental and simulation, the drop in transmittance starts accelerating at 20° with most of the light attenuated by 50°. This establishes 20° as the working angle for a recognizable bend *for this particular sensor*, which we define as the minimum bend angle required to reliably detect a bend. The offset between the experimental and simulation results is due to the simulation optical source not matching the intensity of the experimental source LED.

B. *Gap Length*

Fig. 5c also shows that the effective **bend sensitivity** of the sensor can be changed by changing the gap length, which in turn changes the min working angle. An increase in **gap length** increases the bend sensitivity at the cost of lower transmittance of the entire fiber. This can be alleviated by using a more powerful light source.

TABLE III
OPTIGAP SENSOR SYSTEM PROPERTIES & PARAMETERS

Name	Has An Effect On
Bend Sensitivity	Min bend angle for intensity drop
Diameter	Total transmittance based on light source
Gap Length	Bend sensitivity
Sensing Resolution	Minimum length between gaps

C. Diameter

Simulation results in Fig. 5b show that small cone angles produce the highest transmittance. This suggests that the **diameter** of the light pipe has a direct effect on the optical intensity, and thus maximum sensor distance. Our testing indicates the transmittance can be maximized by using a light source with the smallest possible cone angle if multiple diameter fibers are going to be used, or by matching the light source to the fiber diameter if a single diameter is used for the application.

D. Sensing Resolution

The bend sensitivity also dictates the **sensing resolution** since only one air gap pattern should be bending at a time. We define the sensing resolution simply as the minimum gap-to-gap spacing. Our testing suggests that $5\,\mathrm{cm}$ is a reasonable resolution for most materials.

E. Full System and Classifier Performance

After validating the model and gaining a better understanding of the effects of various properties on transmittance, we validated the full OptiGap sensor system. To make the system easily usable and reconfigurable, we developed a GUI (Fig. 7) that enables quick data gathering from the sensors, interactive data labeling, and model fitting. We performed initial tests of hand bending the sensor and verifying the classification. For repeatability, we created an automated bending rig (Fig. 6d) consisting of a tape spring arm with a servo on one end and a free-spinning shaft on the other end.

Results (Fig. 6d) show the output tracked with the location of the bend along the arm, showing the bend-sensitive areas and the non-sensitive areas. While there is no single accuracy metric for the system as a whole since that is entirely dependent on the fitting and fabrication of a particular configuration, this configuration tested had a 100% accuracy measure. However, one potential source of error is little separation between low and high signal levels, which can occur if the gap lengths are too large, resulting in transmittance below a usable threshold. Using the STM32 running at $100\,\mathrm{Mhz}$, the sensor was outputting data at $175\,\mathrm{Hz}$ using a UART baud rate of 115200.

F. Sensor Attachment

We explored various techniques for attaching the sensors to mechanisms, including tapes such as masking, painter's, fabric, and polyimide tape. Polyimide tape was the most versatile especially when sticking the sensor to our tape spring test station. Other techniques included using flexible but stabilizing material like a thin PET sheet shown in Fig. 6b as well as flexible silicone adhesives. Since the motivating factor around the development of the OptiGap system was to have a sensor that could sense the bending of the TASL in [1], we are exploring ways of embedding the sensor into the surface of materials. As Seen in Fig. 6c, we used a ZSK tailored wire placement machine to sew fibers for an OptiGap sensor into a fabric material much like the TASL. Once we validate this technique, we can embed an OptiGap sensor directly into the TASL during fabrication.

G. Underwater Sensing

To demonstrate the versatility of the sensor system, we fabricated a sensor using off-the-shelf clear TPU 3D printer filament as the light pipe. This provided an opportunity to test the performance of the sensor system underwater. The sensor, shown in Fig. 6a, had no change in performance when submerged vs in free air, which raises the potential for use in underwater robotics.

H. Limitations

The primary limitation of the OptiGap system is that it currently can only detect bending at one location at a time, which stems from its basis as a linear encoder. Because OptiGap uses a GNB classifier, it is possible for the sensor to be fooled into thinking a bend is occurring at a particular location when multiple air gap patterns are bent at once. This limits applications to those of linear encoders but with the advantage of being customizable, compliant, and usable in wet conditions. The second limitation, common to all soft optical sensors, is the inability of the sensor to work in very high-temperature environments due to the risk of melting the fibers.

IV. CONCLUSION AND FUTURE WORK

In this paper, we presented and demonstrated the OptiGap sensor system, a novel bend localization system that is low cost, flexible, simple to fabricate, able to perform real-time bend localization, and can work on any modern microcontroller. We also presented and verified through simulation and experimentation the approach of using an air gap with a flexible sleeve to create bend-sensitive air gap patterns in a light pipe. This sensor system has the potential for use in many robotics and automation systems that require flexibility, reconfiguration, and noise immunity – this includes underwater conditions. The ability to use various light pipe materials with the same sensor system based on the application puts the OptiGap system at a heightened advantage over other sensors. The ultimate goal for this sensor system is to integrate the processing into a small custom hardware package and create a more robust software package and toolchain for the automated fitting of new sensor patterns.

REFERENCES

[1] P. Bupe, D. J. Jackson, and C. K. Harnett, "Electronically reconfigurable virtual joints by shape memory Alloy-Induced buckling of curved sheets," in *SoutheastCon 2022*, pp. 598–604, Mar. 2022.

[2] Y. Jiang, M. Sharifzadeh, and D. M. Aukes, "Reconfigurable soft flexure hinges via pinched tubes," in *2020 IEEE/RSJ International Conference on Intelligent Robots and Systems (IROS)*, pp. 8843–8850, ieeexplore.ieee.org, Oct. 2020.

[3] M. Jiang, Q. Yu, and N. Gravish, "Vacuum induced tube pinching enables reconfigurable flexure joints with controllable bend axis and stiffness," in *2021 IEEE 4th International Conference on Soft Robotics (RoboSoft)*, pp. 315–320, Apr. 2021.

[4] Y. Jiang, M. Sharifzadeh, and D. M. Aukes, "Shape change propagation through soft curved materials for Dynamically-Tuned paddling robots," in *2021 IEEE 4th International Conference on Soft Robotics (RoboSoft)*, pp. 230–237, Apr. 2021.

[5] M. Sharifzadeh and D. M. Aukes, "Curvature-Induced buckling for Flapping-Wing vehicles," *IEEE/ASME Transactions on Mechatronics*, vol. 26, pp. 503–514, Feb. 2021.

[6] Eid, "Optical fiber sensors: review of technology and applications," *Indonesian journal of electrical engineering and computer science*, 2022.

[7] B. P. Pal, "Optical fiber sensors: A versatile technology platform for sensing," *Journal of the Indian Institute of Science*, vol. 94, pp. 283–310, Sept. 2014.

[8] M. A. Zawawi, S. O'Keeffe, and E. Lewis, "Compensated intensity-modulated optical fibre bending sensor based on tilt angle loss measurement," in *SENSORS, 2014 IEEE*, pp. 370–373, Nov. 2014.

[9] M. A. Zawawi, S. O'Keeffe, and E. Lewis, "An extrinsic optical fiber bending sensor: A theoretical investigation and validation," *IEEE sensors journal*, vol. 15, pp. 5333–5339, Sept. 2015.

[10] J.-T. Lin, C. Newquist, and C. K. Harnett, "Multitouch pressure sensing with soft optical time-of-flight sensors," *IEEE transactions on instrumentation and measurement*, vol. 71, pp. 1–8, 2022.

[11] H. Zhao, R. Huang, and R. F. Shepherd, "Curvature control of soft orthotics via low cost solid-state optics," in *2016 IEEE International Conference on Robotics and Automation (ICRA)*, pp. 4008–4013, May 2016.

[12] C.-Y. Huang, W.-C. Wang, W.-J. Wu, and W. R. Ledoux, "Composite optical bend loss sensor for pressure and shear measurement," *IEEE sensors journal*, vol. 7, pp. 1554–1565, Nov. 2007.

[13] H. Bai, S. Li, J. Barreiros, Y. Tu, C. R. Pollock, and R. F. Shepherd, "Stretchable distributed fiber-optic sensors," *Science*, vol. 370, pp. 848–852, Nov. 2020.

[14] O. U. Lashmanov, A. S. Vasilev, A. V. Vasileva, A. G. Anisimov, and V. V. Korotaev, "High-precision absolute linear encoder based on a standard calibrated scale," *Measurement*, vol. 123, pp. 226–234, July 2018.

[15] Usha and Sankar, "Binary orthogonal code generation for multi user communication using n-bit gray and inverse gray codes," *Archiv fur Elektronik und Ubertragungstechnik [International journal of electronics and communications]*.

[16] D.-M. Pham, A. B. Premkumar, and A. S. Madhukumar, "Error detection and correction in communication channels using inverse gray RSNS codes," *IEEE Transactions on Communications*, vol. 59, pp. 975–986, Apr. 2011.

[17] E. Brookner, *Tracking and Kalman filtering made easy*. New York: Wiley, 1998.

[18] R. O. Duda, P. E. Hart, and D. G. Stork, *Pattern Classification*. John Wiley & Sons, Nov. 2012.